Efficient EM-based variability analysis of passive microwave structures through parameterized reduced-order behavioral models

(Article begins on next page)

20 April 2024

# Efficient EM-based variability analysis of passive microwave structures through parameterized reduced-order behavioral models

C. Ramella[1], A. Zanco[2], M. De Stefano, T. Bradde,M. Pirola,S. Grivet-Talocia

DET - Politecnico di Torino, Italy

{[1]chiara.ramella, [2]alessandro.zanco }@polito.it

*Abstract* — In this contribution we demonstrate how reduced-order behavioral models allow for extremely accurate and computationally efficient electromagnetic-based variability analysis of microwave passive structures. In particular, we report the MonteCarlo analysis of a wideband matching network at Ka-band, designed with a commercial foundry GaN-HEMT process PDK. As sources of variation we considered the thickness of the two dielectric layers available in the PDK to implement MIM capacitors of different order of magnitude, both exploited in the network. Based on a limited set of electromagnetic simulations, a parameterized behavioral model is extracted and then translated into a parameterized circuit equivalent (SPICE netlist) straightforward to be imported into RF CAD tools. The adopted model, implementing a rational approximation of the simulated S-parameters with rational dependence on the two parameters, provides excellent agreement with electromagnetic simulations, robustness against port impedance change and good extrapolation capabilities.

*Keywords* — behavioral modeling, parameterized modeling, microwave circuits, variability analysis

## I. INTRODUCTION

With the advent of the 5G standard, the design of monolithic microwave integrated circuits (MMICs) at Ka-band and above is becoming a hot research topic [1]–[3]. The technological and design challenges posed by adopting high center frequencies are manifold. Among them, process induced variability is rising the attention of microwave designers, since all their efforts in performance optimization can eventually be jeopardized by the MMIC yield. At high frequency, electromagnetic coupling between elements must be accounted for through electromagnetic (EM) simulation and optimization [4], [5]. For the same reason, variability analysis to address performance and yield has to be carried out at EM level adopting the process statistical distributions typically included in the foundries' process design kits (PDKs).

Since EM simulations, even in their most computationally efficient form, are extremely time-consuming, they are typically adopted only for fine tuning, while hardly used for fully-EM-based optimization from scratch and-/or variability analysis capable to accurately account for lumped and distributed element cross-coupling.

Parameterized behavioral models extracted from EM simulations, are the most promising candidates to enable fast and efficient EM-based variability analysis, provided that high accuracy and easy implementation within CAD tools is

guaranteed [6]. For one or few parameters, a look-up-table (LUT) model can be adopted [7], but as the number of parameters increases, the efficiency of such an approach rapidly decreases. Moreover, LUT-based models strongly rely on the interpolation/extrapolation algorithms embedded within the adopted CAD tool, hence limiting the designer's grip and control on their accuracy.

In this work, we demonstrate the application of the parameterized behavioral model presented in [8] for EM-based variability analysis. This model provides a closed-form approximation of the EM-simulated S-parameters as rational functions of frequency and Chebyshev polynomials of the parameters. The mathematical model is then translated into an equivalent circuit, in the form of a SPICE netlist [9], which can be easily imported into practically any CAD tool. This approach to variability analysis, successfully adopted in the framework of polynomial chaos [10], [11], is here is applied for the first time (as far as the author's' knowledge goes) to EM-simulated microstrip networks.

The accuracy of the proposed approach is demonstrated on a wideband matching network around $28\,\mathrm{GHz}$, transforming a highly reflective complex impedance, i.e., a typical optimum output impedance for power of GaN transistors at this frequency, to $50\,\Omega$, including DC-blocks and in-band short-circuited biasing stubs. The network has been designed and EM optimized resorting to the PDK of a commercial GaN-HEMT foundry, which includes also the EM substrate stack-up for 3D-planar EM simulation.

The passive components that are most affected by process variations are the MIM capacitors, implemented through thin layers of dielectric materials. In particular, the selected process provides two different types of MIM capacitor, for implementing smaller (tens of $\mathrm{pF/mm^2}$) or bigger (hundreds of $\mathrm{pF/mm^2}$) capacitance values. The thickness of the two dielectrics adopted for these elements is therefore considered for the statistical analysis, considering variation ranges taken from the statistical data available in the PDK. A relatively small set of EM simulations was sufficient to extract the model and perform, in few minutes, a MonteCarlo analysis with hundreds of trials. The results obtained are in excellent agreement with EM simulations on all the selected test points, considering also some extrapolation margin, proving the validity of the approach for EM-based variability analysis.

## II. TEST-CASE MATCHING NETWORK

The selected test-case network is the output matching of a single, large-periphery GaN transistor at 28 GHz. The optimum impedance for power at the center frequency is ($Z_{\text{Lopt}} = 5.8 + j10.9)\,\Omega$, i.e., a highly reflective load (0.8 magnitude of the reflection coefficient), as shown in Fig. 1a. This value is matched to $50\,\Omega$ through a multi-step semi-lumped pi-type matching network, including a short-circuited stub adopted also for device biasing, a large series DC-block capacitor and two shunt capacitors acting as open-circuited stubs. All elements have been split into parallel pairs to achieve a symmetric layout as shown in Fig. 1a. Adopting the complex conjugate of the optimum load, $Z_{\text{Lopt}}^*$ as reference impedance at the input port, a matching better than -20 dB is achieved in the 25 GHz - 33 GHz range, as shown in Fig. 1b. The matching network adopts both large (as RF-short and DC-block) and small (as open-circuited stubs) MIM capacitors. The former are implemented through a thin silicon nitride layer (around 150 nm) while the latter exploit also an additional oxide layer (around 800 nm). Compatibly with available statistical data, the relative standard deviation (assuming gaussian distribution) for the two layer thicknesses has been set to 5% and 3%, respectively. Only a $\pm\sigma$ variation around the nominal value has been considered to fix the parameter space boundaries adopted for model extraction, so as to assess also its extrapolation capabilities during the MonteCarlo analysis.

## III. BEHAVIORAL PARAMETERIZED MODEL

The adopted (frequency-dependent) parameterized model structure $\mathbf{H}(s, \boldsymbol{\vartheta})$ is based on the well-established [12] rational barycentric form

$$\mathbf{H}(s, \boldsymbol{\vartheta}) = \frac{\sum_{n=0}^{\bar{n}} \mathbf{R}_n(\boldsymbol{\vartheta})\varphi_n(s)}{\sum_{n=0}^{\bar{n}} r_n(\boldsymbol{\vartheta})\varphi_n(s)}, \qquad (1)$$

where $s = j2\pi f$ is the complex angular frequency, and $\boldsymbol{\vartheta}$ is the parameter vector, in this case containing 2 parameters, i.e. $\boldsymbol{\vartheta} = [\vartheta_1, \vartheta_2]$, corresponding to thickness of the nitride and oxide layers. The parameterized numerator and denominator coefficients are further expanded as linear combination of suitable parameter basis functions $\xi_\ell(\boldsymbol{\vartheta})$, as

$$\mathbf{R}_n(\boldsymbol{\vartheta}) = \sum_\ell \mathbf{R}_{n,\ell}\xi_\ell(\boldsymbol{\vartheta}), \quad r_n(\boldsymbol{\vartheta}) = \sum_\ell r_{n,\ell}\xi_\ell(\boldsymbol{\vartheta}) \qquad (2)$$

The frequency dependence is embedded in the model through the basis functions $\varphi_n(s) = 1/(s - q_n)$, that are defined on a set of predefined basis poles $q_n$ if $n > 0$ and $\varphi_n(s) = 1$ if $n = 0$. Conversely, the choice of the basis functions $\xi_\ell(\boldsymbol{\vartheta})$ is quite free; depending on the problem at hand, several possibilities have been explored [13], [14]. In this work, we will use multivariate Chebyshev polynomials.

Based on the variability estimates of Section II, we assume that the thickness of each layer attains values $\vartheta_i$ that are uniformly bounded in the range $[\underline{\vartheta}_i, \bar{\vartheta}_i]$, $i = 1, 2$. More formally, we define the parameter space $\Theta$ as the Cartesian product

$$\Theta = [\underline{\vartheta}_1, \bar{\vartheta}_1] \times [\underline{\vartheta}_2, \bar{\vartheta}_2] \qquad (3)$$



(a) Layout.
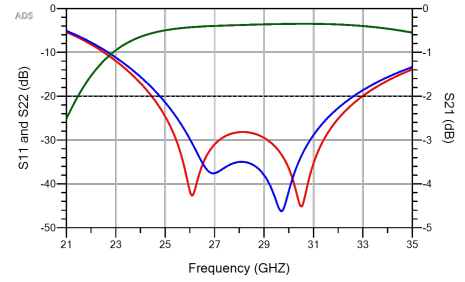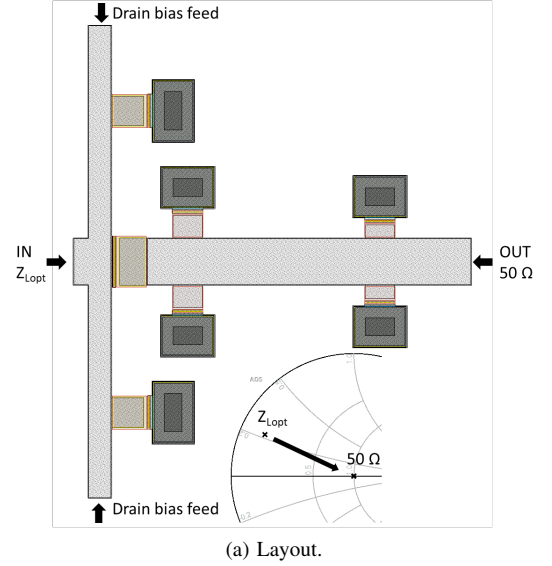


(b) Matching performance.

Fig. 1. Layout (a) and performance (b) of the designed matching network in the 21 GHz - 35 GHz range. Legend: $S_{11}$ =red, $S_{21}$ =green and $S_{22}$ =blue.

containing all the possible combinations of layer thicknesses.

Based on the parameterized model form (1), we want to optimize the numerator and denominator coefficients $\mathbf{R}_{n,\ell}$, $r_{n,\ell}$ so that the model accurately reproduces the broadband behavior of the network, for all the combination of layer thicknesses.

To this end, the first step is to gather a limited (yet, relevant) set of electromagnetic scattering responses $\breve{\mathbf{S}}(j\omega_k, \boldsymbol{\vartheta}_m)$, $k = 1, \ldots, K$, $m = 1, \ldots, M$, of the network at selected combinations of parameter values. The EM simulations have been performed with Keysight Momentum, considering a 20 GHz bandwidth around 28 GHz (sampled linearly with 100 MHz step) and a 40 cells/wavelength mesh at 100 GHz mesh frequency, yielding to roughly 3000 mesh nodes. It is worth to note that EM simulations, hence model extraction, are referred to a normalization impedance of $50\,\Omega$ at both ports. To better control the model-data error over the whole parameter space, we assume these raw data-samples to be uniformly distributed in $\Theta$.

Then, the model coefficients are estimated by solving the non-linear optimization problem

$$\mathbf{H}(s_k, \boldsymbol{\vartheta}_m) - \breve{\mathbf{S}}(j\omega_k, \boldsymbol{\vartheta}_m) \approx \mathbf{0} \quad \forall k, m \qquad (4)$$

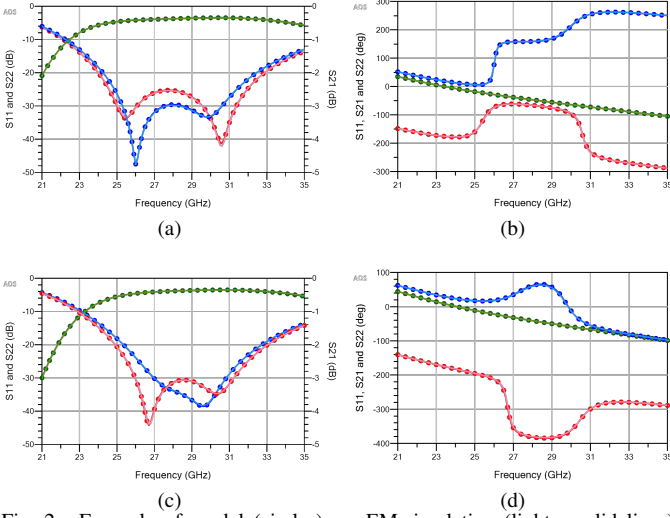through the so-called *Parameterized Sanathanan-Koerner*

Fig. 2. Example of model (circles) vs. EM-simulation (lighter solid lines) results at 2 extraction points: (a)-(b) both nominal-$\sigma$ (c)-(d) both nominal+$\sigma$. Legend: $S_{11}$ =red, $S_{21}$ =green and $S_{22}$ =blue.



Fig. 3. RMS error of (a) $|S_{11}|$ and (b) $|S_{22}|$ at all extraction (blue crosses) and test (red circles) points.



(a) Matching at input port.  (b) Matching at output port.



(c) Transmission losses.

Fig. 4. Results of the MonteCarlo analysis. Black lines are nominal responses.

algorithm [8]. We remark that the model accuracy is controlled only at the reference impedance of $50\,\Omega$; indeed, the possibility of arbitrarily changing the port reference without affecting the model accuracy is a non-trivial matter in behavioral modeling, as it can introduce uncontrolled error magnifications. Some techniques have been proposed in the context of non-parameterized modeling [15], but no parameterized counterparts are available up to date.

Once the parameterized model $\mathbf{H}(s, \boldsymbol{\vartheta})$ is available, it has been shown in [9] that the conversion to an equivalent parameterized SPICE netlist is possible, enabling the use of surrogate parameterized models in most CAD tools.

## IV. MODEL VALIDATION AND VARIABILITY ANALYSIS

The generated circuit equivalent model has been imported into the RF CAD (Keysight ADS in this case, but the procedure can be extended to any other) as a SPICE netlist. For model extraction, the worst-case RMS error, evaluated over all the available frequency range and parameter data-samples, in reproducing the EM S-parameters was as low as $8.4 \cdot 10^{-4}$. However, it has already been remarked that the same model accuracy is not automatically guaranteed when adopting different ports terminations ($Z^*_{\text{Lopt}}$ at the input in this case). Thus, the very first model validation step consisted in simulating it adopting these modified port reference impedances, but on the same set of parameter values used for extraction. Despite being the selected $Z^*_{\text{Lopt}}$ value very far from $50\,\Omega$, the agreement between the model and the EM-S-parameter results is nearly perfect, as shown in Fig. 2 and Fig. 3 (blue crosses). The root-mean-square (rms) error remains below $1 \cdot 10^{-3}$ for all extraction points.

A MonteCarlo analysis with 500 trial has been then performed considering uncorrelated variations of the two parameters, adopting a gaussian distribution for both with relative variance of 5% (nitride thickness) and 3% (oxide thickness), respectively. Such an analysis, if carried out
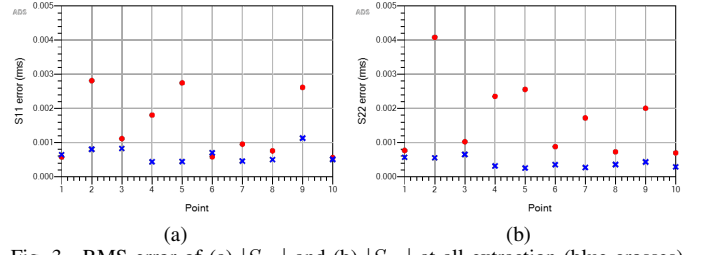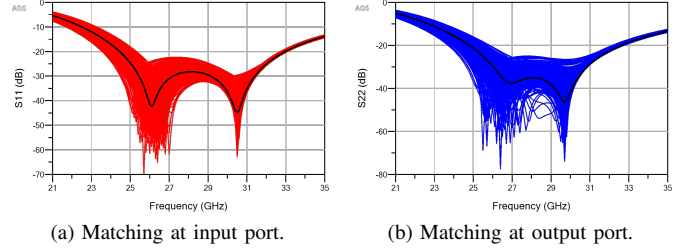
with repeated EM-simulations on a standard, but yet high-performance personal computer, would have required days of simulations while it took less than a minute by resorting to the proposed approach. The results are shown in Fig. 4, showing a significant spread in the lower portion of the band, both in terms of matching and losses.

From the MonteCarlo analysis, 10 combinations of parameter values have been selected as test-points for final model validation, selecting also values outside the boundaries of the extraction parameter space. The agreement between the model results and the EM simulations at the test points is again excellent, as shown in Fig. 5 and Fig. 3 (red circles). The rms error remains within $4 \cdot 10^{-3}$ at all test points, demonstrating the high accuracy of the model and its suitability for variability analysis of microwave passive circuits.

Extrapolation capability of the model has been further tested by comparing it to the EM simulations adopting a larger variation of both parameters, namely $\pm 3\sigma$. The results of this simulations are reported in Fig. 6. As can be noticed, here some discrepancies between the model and the EM results start arising, resulting in a rms error up to $9 \cdot 10^{-3}$. Even if well outside a reasonable extrapolation range, the $\pm 5\sigma$ case has been also tested: the general shape of the response in frequency is still correct, but in this case, the accuracy in predicting the frequency at which negative peaks occur is lost, with up to $700\,\text{MHz}$ discrepancy in the worst case, shown in Fig. 7, where
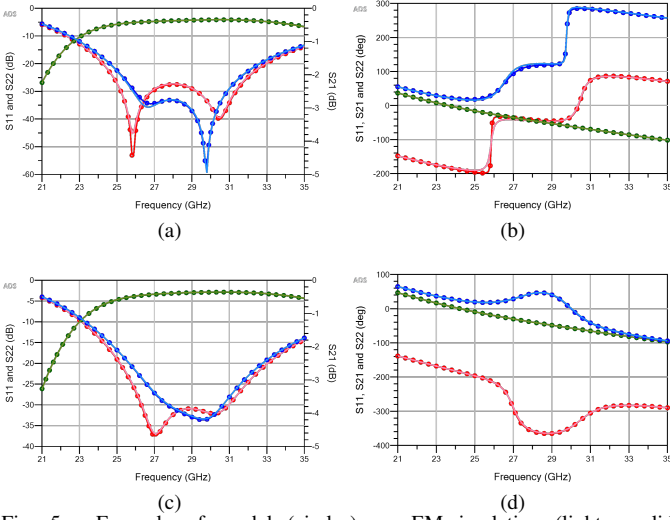
Fig. 5. Example of model (circles) vs. EM-simulation (lighter solid lines) results at 2 test points: (a)-(b) both parameters within the extraction range (c)-(d) both parameter outside the extraction range (+8% and +5%, respectively.). Legend: $S_{11}$ =red, $S_{21}$ =green and $S_{22}$ =blue.
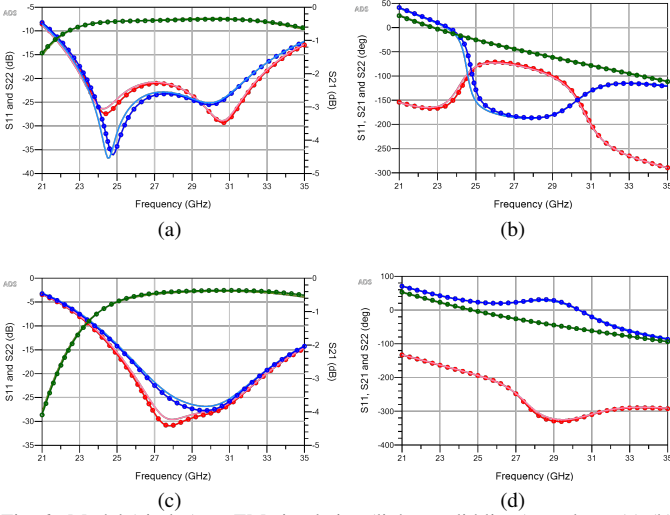


Fig. 6. Model (circles) vs. EM-simulation (lighter solid lines) results at (a)-(b) +3$\sigma$ (c)-(d) −3$\sigma$. Legend: $S_{11}$ =red, $S_{21}$ =green and $S_{22}$ =blue.
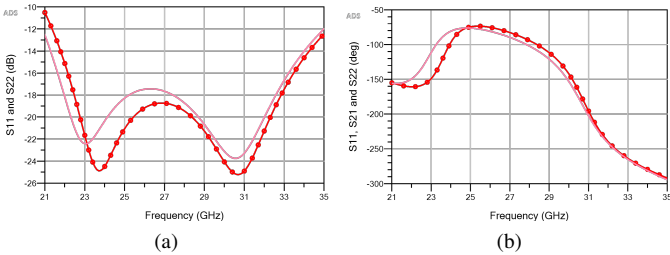


Fig. 7. Model (circles) vs. EM-simulation (lighter solid lines) results at +5$\sigma$. Only $S_{11}$ = is reported as it show the worst agreement.

the rms error grows to $3.5 \cdot 10^{-2}$.

## V. CONCLUSION

We presented a computationally efficient approach for EM-based variability analysis based on behavioral

parameterized surrogate models. The latter are constructed starting from a reduced set of scattering responses at distinct instances of the parameters of interest. The model is then converted into an equivalent parameterized SPICE netlist, which enables its use in CAD tools. The procedure has been validated through a MonteCarlo analysis of a wideband matching network at Ka-band. The results demonstrate the accuracy of the equivalent parameterized model, that can be efficiently used in place of extremely time-demanding EM-solver runs. The model proved to be accurate despite port impedance change, also in unexplored regions of the parameter space, hence showing remarkable extrapolation capabilities.

## REFERENCES

[1] R. Giofrè, A. Del Gaudio, and E. Limiti, "A 28 GHz MMIC Doherty Power Amplifier in GaN on Si Technology for 5G Applications," in *Proc. IMS 2019*, 2019, pp. 611–613.

[2] S. Zhang *et al.*, "An 18–31-GHz GaN-Based LNA With 0.8-dB Minimum NF and High Robustness," *IEEE Microw. Wireless Compon. Lett.*, vol. 30, no. 9, pp. 896–899, 2020.

[3] M. Bao *et al.*, "A 24–28-GHz Doherty Power Amplifier With 4-W Output Power and 32% PAE at 6-dB OPBO in 150-nm GaN Technology," *IEEE Microw. Wireless Compon. Lett.*, vol. 31, no. 6, pp. 752–755, 2021.

[4] P. Neininger *et al.*, "Design, analysis and evaluation of a broadband high-power amplifier for ka-band frequencies," in *Proc. IMS 2019*, 2019, pp. 564–567.

[5] C. Ramella *et al.*, "Electro-magnetic Crosstalk Effects in a Millimeter-wave MMIC Stacked Cell," in *Proc. INMMiC 2020*, 2020, pp. 1–3.

[6] S. Donati Guerrieri *et al.*, "Bridging the gap between physical and circuit analysis for variability-aware microwave design: Modeling approaches," *El.*, vol. 11, no. 6, 2022.

[7] ——, "Efficient sensitivity and variability analysis of nonlinear microwave stages through concurrent TCAD and EM modeling," *IEEE J. Multiscale Multiphys. Comput. Tech.*, vol. 4, pp. 356–363, 2019.

[8] P. Triverio, S. Grivet-Talocia, and M. S. Nakhla, "A parameterized macromodeling strategy with uniform stability test," *IEEE Trans. Adv. Packag.*, vol. 32, no. 1, pp. 205–215, Feb 2009.

[9] S. Grivet-Talocia and R. Trinchero, "Behavioral, parameterized, and broadband modeling of wired interconnects with internal discontinuities," *IEEE Transactions on Electromagnetic Compatibility*, vol. 60, no. 1, pp. 77–85, 2018.

[10] Y. Ye *et al.*, "A comprehensive and modular stochastic modeling framework for the variability-aware assessment of signal integrity in high-speed links," vol. 60, no. 2, pp. 459–467, 2018.

[11] P. Manfredi and F. G. Canavero, "Efficient statistical simulation of microwave devices via stochastic testing-based circuit equivalents of nonlinear components," *IEEE Trans. Microw. Theory Techn.*, vol. 63, no. 5, pp. 1502–1511, 2015.

[12] Deschrijver, Dirk and Dhaene, Tom and De Zutter, Daniël, "Robust parametric macromodeling using multivariate orthonormal vector fitting," *IEEE Trans. Microw. Theory Techn.*, vol. 56, no. 7, pp. 1661–1667, 2008. [Online]. Available: http://dx.doi.org/1854/12612

[13] S. Grivet-Talocia and E. Fevola, "Compact parameterized black-box modeling via Fourier-rational approximations," vol. 59, no. 4, pp. 1133–1142, 2017.

[14] A. Zanco *et al.*, "Uniformly stable parameterized macromodeling through positive definite basis functions," *IEEE Trans. Compon. Packag. Manuf. Technol.*, vol. 10, no. 11, pp. 1782–1794, 2020.

[15] B. Gustavsen, "Fast passivity enforcement for pole-residue models by perturbation of residue matrix eigenvalues," *IEEE Trans. Power Del.*, vol. 23, no. 4, pp. 2278–2285, 2008.